Electromagnetic Fields in Electrical Engineering
vol. 22, pp. 190-195, IOS Press, 2002
Editors A. Krawczyk and S. Wiak
ISBN 1 58603 232 1 - ISSN 1383-7281

PARAMETRIC STUDY OF ROTOR SLOT SHAPE ON A CAGE INDUCTION MOTOR

Vicente Aucejo Galindo[1], Xose M. López-Fdez[2], J.A. Dias Pinto[3] and A. Paulo Coimbra[4]

[1]INDIELEC - Ingeniería de Diseño Electrotécnico, Valencia – Spain, vaucejo@indielec.es
[2]Dept. of Electrical Engineering, Vigo University – Spain, xmlopez@ieee.org
[3]ISR/Instituto Superior de Engenheria de Coimbra (ISEC), Coimbra – Portugal, j.pinto@ieee.org,
[4]ISR/Dept. of Electrical Engineering, Coimbra University – Portugal, acoimbra@dee.uc.pt

Abstract - **In this work the use of the parameterisation in the study of the geometric redesign of the rotor slots on a cage induction motors is presented. A magnetodynamic model of finite elements was developed in order to obtain new performance curves. The results are obtained from an industrial 90-kW 4-pole three-phase double-squirrel cage motor.**

Introduction

Usually the rotor slots geometry can be considered as an independent design parameter [1]. Nowadays, with the computing tools based on the numerical analysis, it is possible the redesigning of the rotor slots to improve the electromagnetic performance of squirrel cage induction motors without significant cost [2]. Therefore, formal methods can be adequate to modify geometric parameters of the rotor slots until the optimal performance is achieved.

This work presents the results of a parametric study of the geometry of the rotor slots on an 4-pole three-phase double-squirrel cage large induction motor. For this purpose a magnetodynamic model using a finite element software package was developed [3]. In the implementation of the model it was taken into account both the presence of external circuits supplied by voltage sources as well as the motor's end-rings resistance and inductance [4].

Description of the problem

The aim of the present work is to improve the performance of a previous motor design at starting while the nominal performance is maintained. This is accomplished by increasing locked-rotor torque and lowering locked-rotor current.

In fact, the rotor resistance has the effect of shaping the speed-torque curve, which is largely independent of stator design [1]. If the cross-section area of the end-rings is limited by mechanical restrictions, the rotor bar resistance offers the possibility to adjust the rotor tooth width as well as the rotor depth below the slot [2]. In order to achieve this goal, the numeric approach proposed by the authors is to seek the improved performance by redesigning the rotor slots. This is performed by automatically modifying the parameterised geometry within a given rotor bar cross-sectional area.

Strategy to parameterise the rotor slot

Some insights into the possibilities for redesigning rotor slots may be gained by considering their cross-sectional areas [2]. To explore this, the expression for output power can be examined:

$$P_{out} = \frac{3 I_2^{'2} R_2^{'} \omega_r}{s \omega_s} \tag{1}$$

Electromagnetic Fields in Electrical Engineering
vol. 22, pp. 190-195, IOS Press 2002
Editors A. Krawczyk and S. Wiak
ISBN 1 58603 232 1 - ISSN 1383-7281

Where R'_2 is the rotor resistance and I'_2 is the rotor current, both referred to the stator, ω_s is the angular frequency of the stator supply, ω_r is the angular frequency of the rotor and s is the slip.

At nominal load, the rotor resistance is approximately proportional to the inverse of the bar cross-sectional area, if the end-rings resistance is neglected. Consequently the following expression will arise:

$$A_b \left(\frac{\sigma}{l_b} s_n \right) \approx \frac{s_n}{R'_2} = \frac{3 I'^2_2 \ \omega_r}{P_{out} \ \omega_s} \tag{2}$$

Where s_n is the nominal load slip, l_b is the length of the bar, σ is the aluminium conductivity and A_b is the total bar cross-sectional area. If the number of the poles, supply frequency, voltage and output power do not change, then the terms on the right-hand side of equation (2) are practically constant. Therefore, in order to maintain the performance under nominal load the following is considered:

$$A_b \approx constant \tag{3}$$

Another important consideration with double-cage is the role that the top slot plays on locked-rotor skin-depth, and consequently on the locked-rotor torque value. With the locked-rotor the torque is approximately given by equation (4).

$$T_o \approx \frac{3 I_o^2 R'_{2o}}{\omega_s} \tag{4}$$

Where R'_{2o} is the locked-rotor resistance and I'_0 is the locked-rotor current, both referred to the stator. Neglecting rotor end-rings, R'_{2o} is inversely proportional to the locked-rotor skin-depth area $A_{b\delta}$. So it yields:

$$\frac{A_{b\delta} T_o}{I'^2_o} \approx constant$$

From the above description, $A_{b\delta}$ must be decreased in order to increase the locked rotor torque and decrease the locked rotor current. Meanwhile, the total cross-sectional area A_b, must be practically constant in order to keep the nominal performance.

Parameterisation of the rotor slot

The parameterisation of the rotor slot is based on the previous slot shape shown in Fig.1. The chosen geometric parameters are: the radius r_1, r_2 and r_3, the width w_1, and the depths d_1, d_2 and d_3.

The authors have adopted a compromise between the need to optimise the slot shape and the time required to perform this study. According with this time constrains, the depths (d_1,d_2), the width (w_1) and the radius (r_3) are deemed to be fixed. So, the *AREA_3* should be a constant value and there are three possible variable parameters to redesign the slot (r_1, $\boldsymbol{r_2}$, $\boldsymbol{d_3}$). The radius r_1 is chosen as a parameter dependent on the depth d_3 and on the radius r_2 by means of the *AREA_1* value (see Fig.1), since the total cross-sectional area of the slot A_b should be a constant value. From the mentioned, a relationship between cross-sectional areas is obtained:

$$AREA\_1 = Ab - (AREA\_2 + AREA\_3) = Ab - ((0.5\ \pi (\boldsymbol{r_2}^2 + r_3^2) + (\boldsymbol{r_2} + r_3)\ \boldsymbol{d_3}) + AREA\_3) \tag{5}$$

Electromagnetic Fields in Electrical Engineering
vol. 22, pp. 190-195, IOS Press 2002
Editors A. Krawczyk and S. Wiak
ISBN 1 58603 232 1 - ISSN 1383-7281

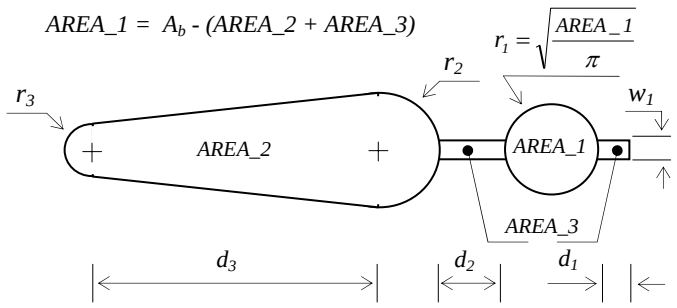

Fig.1. Geometric parameterisation.

The depth d_3 and the radius r_2 are finally two independent parameters, which are used in the following sections.

Model of the motor

Nowadays, the used numerical methods and mainly FEA allow to simulate the influence of the rotor´s geometrical parameters on motor's performance characteristics. FEM offers the possibility of relating the global electrical, mechanical and local electromagnetic quantities, with a particular geometric shape.

In this work, a 2D finite elements software package (Flux2D) was employed to simulate the magnetodynamic performance of the motor. The motor's voltage supply is modelled by an external circuit also taking into account the rotor squirrel cage characteristics [3].

Field model of the induction motor

The magnetic field of the induction motor is computed using a 2D FEM and assuming an AC non-linear problem [4]. This approach enables to study the influence of the rotor bars geometric shape on the motor`s operating characteristics (torque and current vs. slip). The electromagnetic field model in the magnetodynamic problems is based on the Maxwell's equations and on the concept of magnetic vector potential. As known, in 2D problems the diffusion equation (6) provides the means to calculate the induced bar currents in the rotor cage.

$$\nabla \times \left(\frac{1}{\mu} \nabla \times A \right) = -j s \omega_s \sigma A + J \tag{6}$$

Where A is the magnetic vector potential (unknown), σ is the electrical conductivity, ω_s is the angular frequency of the stator supply, s is the slip, μ is the magnetic permeability and J is the current density supplied by external voltage sources.

The natural excitation for finite element models is usually a current (or current density). In the real motor the current is normally unknown since it is supplied by an external electric circuit. Therefore, the external electric circuit which supplies with voltage V must be modelled as coupled to the 2D FE model [4].

The current i in a stranded coil of the field model can be expressed as follows :

$$i = \frac{\sigma}{2N l_c} \left[S \left(V - R_{et} i + L_{e_t} \frac{di}{dt} \right) - S e \right] \tag{7}$$

Electromagnetic Fields in Electrical Engineering
vol. 22, pp. 190-195, IOS Press 2002
Editors A. Krawczyk and S. Wiak
ISBN 1 58603 232 1 - ISSN 1383-7281

Where R_{et} is the end-turn resistance, L_{et} is the end-turn inductance, N is the coil turns, S is the cross-sectional area where i flows, l_c is the length of the strand coil and e is the induced e.m.f. on the strand coil. This induced e.m.f. on a coil (S^+,S^-) can be expressed as follows:

$$e = \frac{l_c}{S}\left(\iint_{S^+} \frac{\partial A}{\partial t}\ \partial S - \iint_{S^-} \frac{\partial A}{\partial t}\ \partial S \right) \tag{8}$$

Geometry of the model

In order to reduce the computation time it is necessary to apply Dirichlet and Neumann conditions taking into account the symmetries of the geometry as well as the field periodicity that arises in the rotating electrical machines. Fig.2 (a) shows the outline of the problem which corresponds to one pole pitch.

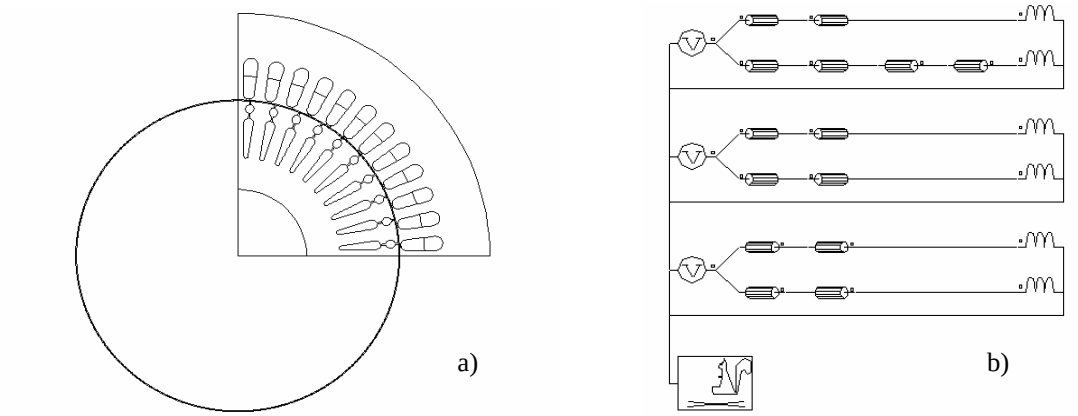

Fig.2 a) Geometry of the model. b) Electric circuit model.

External electric circuit

The used electromagnetic field model considers a coupling to an external electric circuit in order to represent the external voltage sources. Fig.2 (b) shows the external electrical connections used for the induction motors. Each horizontal branch represents the respective active conductors of a coil of a phase winding. These elements are modelled including winding turns and the resistance to relate with the region in the domain of finite elements. The inductance which appear in the external circuit represents the correspondent front and back end-turns of each coil. The related circuit shows one pole pitch. The symbolic squirrel cage is a macro component that Flux2D model including solid conductors to represent the rotor bars and the end-rings resistance and end rings inductance.

Practical application

The manufacturer's motor characteristics are presented in Table I. Flux2D software package allows to create parameterised geometry in two dimensions and a finite element mesh in an entirely interactive way. The finite element mesh used in this study has 12500 nodes and 6800 second order elements, see Fig.3 (a). This mesh is the result of the combination of triangular and quadrilateral elements. Fig.3 (b) shows the five slot shapes analysed considering different values for the two variable geometric parameters (r_2, d_3) shown in Table II.

Electromagnetic Fields in Electrical Engineering
vol. 22, pp. 190-195, IOS Press 2002
Editors A. Krawczyk and S. Wiak
ISBN 1 58603 232 1 - ISSN 1383-7281

Table I. Motor characteristics.

Power (kW)	90
Line voltage (V)	400
Line current (A)	168
Connection type	Y
Frequency (Hz)	50
Number of poles	4
Number of stator slots	48
Number of rotor bars	40
Efficiency	95 %
Power factor	0.83

Table II. Values of the variable geometric parameters.

Rotor slot types		$\mathbf{r_2}$	$\mathbf{d_3}$	r_1
Original	(0)	4.005 mm	29 mm	4 mm
(+) Increment $\mathbf{d_3}$	$(+d_3)$	4.005 mm	(29+4) mm	2.944 mm
(–) Decrement $\mathbf{d_3}$	$(-d_3)$	4.005 mm	(29–4)mm	4.824 mm
(+) Increment $\mathbf{r_2}$	$(+r_2)$	(4.005+0.5) mm	29 mm	3.721 mm
(–) Decrement $\mathbf{r_2}$	$(-r_2)$	(4.005–0.5) mm	29 mm	4.225 mm

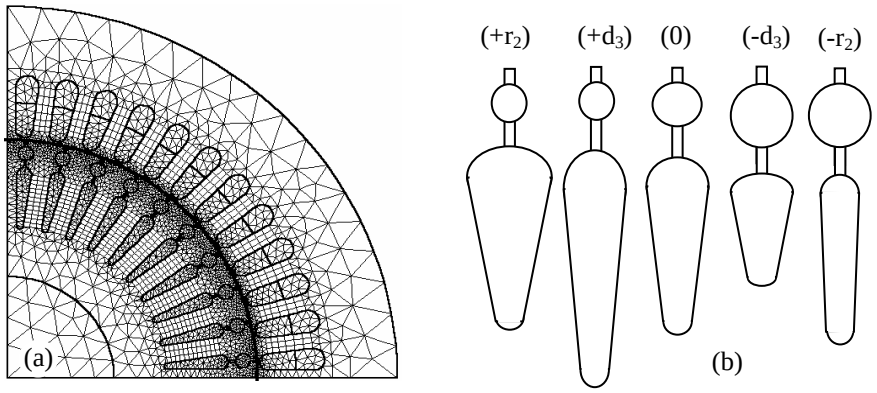

Fig.3. a) Mesh of the model. b) Resultant slots with the Table II values.

Results

Fig.4 shows the magnetic flux lines distribution at locked-rotor starting and under nominal load. Fig.5 shows the results of the numerical simulation (electromagnetic torque and the rotor bar current vs. slip characteristics) for different slip values (from 0 up to 1). To evaluate the torque the virtual work method was used.

Electromagnetic Fields in Electrical Engineering
vol. 22, pp. 190-195, IOS Press 2002
Editors A. Krawczyk and S. Wiak
ISBN 1 58603 232 1 - ISSN 1383-7281

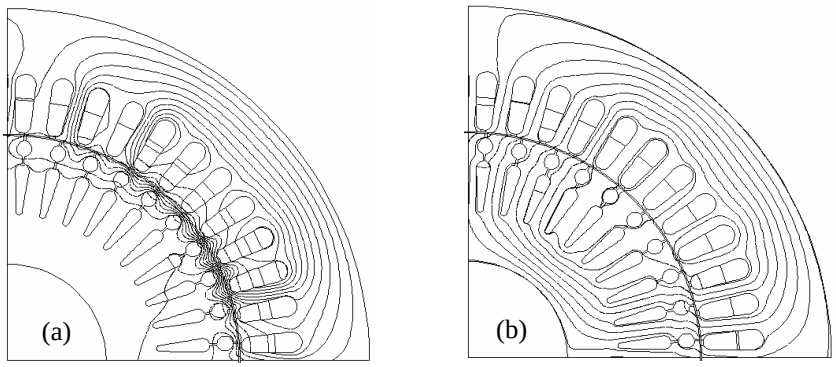

Fig.4. Equiflux distribution a) At locked-rotor starting. b) At nominal load.

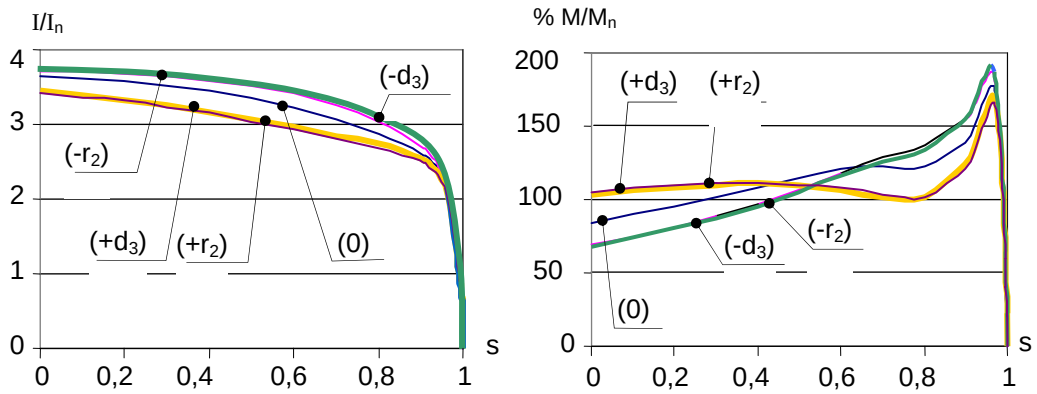

Fig.5. Numerical results vs. slip. a) Stator current p.u. b) Torque, percent of rated full-load torque.

Conclusions

In this paper it has been described a strategy to parameterise geometrically the rotor slot shape. It has been applied on a large double-squirrel cage induction motor in order to seek to improve performance of the motor at starting by redesigning the rotor slots shape. The described strategy shows an easy way to implement the redesign of the rotor slot shape without manufacture additional cost.

The paper has outlined the capability of the actual computing tools based on 2D finite elements coupled to electrical circuit model taking into account 3D effects, as well as the external supply voltage sources.

References

[1] R. H. Engelmann and W. H. Middendorft, "Handbook of Electric Motors", New York: Marcel Dekker, 1995.

[2] Stephen Williamson and Catherine I. McClay. "Optimization of the Geometry of Closed Rotor Slots for Cage Induction Motors, "IEEE Trans. on Industry Applications, vol. 32, no. 3, pp. 560-568, May/June 1996.

[3] FLUX User's guide. Cedrat, Meylan. France 2001.

[4] K. Hameyer and R. Belmans, "Numerical Modelling and Design of Electrical Machines and Devices", Boston: WIT Press, 1999.